PROCEEDINGS OF SCIENCE

The multi-frequency behaviour of Blazars

Elisabetta Cavazzuti
Italian Space Agency (ASI), Italy
Agenzia Spaziale Italiana (ASI) Science Data Center, I-00044 Frascati (Roma), Italy
E-mail: elisabetta.cavazzuti@asi.it

Paolo Giommi*
Italian Space Agency (ASI), Italy
E-mail: paolo.giommi@asi.it

Sara Cutini
Agenzia Spaziale Italiana (ASI) Science Data Center, I-00044 Frascati (Roma), Italy
E-mail: sara.cutini@asdc.asi.it

Andrea Tramacere
ISDC, Data Centre for Astrophysics, Chemin d'Ecogia 16, CH-1290 Versoix, Switzerland
E-mail: andrea.tramacere@unige.ch

Silvia Rainò
Istituto Nazionale di Fisica Nucleare, Sezione di Bari, 70126 Bari, Italy
E-mail: silvia.raino@ba.infn.it

on behalf the Fermi-LAT collaboration

PoS(extremesky2009)040

PROCEEDINGS OF SCIENCE

We have conducted a detailed investigation of the broad-band spectral properties of the γ-ray selected blazars of the *Fermi* LAT Bright AGN Sample (LBAS). By combining our accurately estimated *Fermi* γ-ray spectra with *Swift*, radio, infra-red, optical and other hard X-ray/γ-ray data, collected within three months of the LBAS data taking period, we were able to assemble high-quality and quasi-simultaneous Spectral Energy Distributions (SED) for 48 LBAS blazars. The SED of these γ-ray sources is similar to that of blazars discovered at other wavelengths, clearly showing, in the usual Log ν – Log ν F_ν representation, the typical broad-band spectral signatures normally attributed to a combination of low-energy synchrotron radiation followed by inverse Compton emission of one or more components. We have used these SEDs to characterize the peak intensity of both the low and the high-energy components. The results have been used to derive empirical relationships that estimate the position of the two peaks from the broad-band colors (i.e. the radio to optical, α_{ro}, and optical to X-ray, α_{ox}, spectral slopes) and from the γ-ray spectral index. We find that the γ-ray spectral slope is strongly correlated with the synchrotron peak energy and with the X-ray spectral index, as expected at first order in synchrotron - inverse Compton scenarios. However, simple homogeneous, one-zone, Synchrotron Self Compton (SSC) models cannot explain most of our SEDs, especially in the case of FSRQs and low energy peaked (LSP) BL Lacs. More complex models involving External Compton Radiation or multiple SSC components are required to reproduce the overall SEDs and the observed spectral variability. While more than 50% of known radio bright high energy peaked (HSP, HBL in the old BL Lac nomenclature) BL Lacs are detected in the LBAS sample, only less than 13% of known bright FSRQs and LSP BL Lacs are included. This suggests that the latter sources, as a class, may be much fainter γ-ray emitters than LBAS blazars, and could in fact radiate close to the expectations of simple SSC models.

The Extreme sky: Sampling the Universe above 10 keV
October 13-17 2009
Otranto (Lecce) Italy

*Speaker.

PoS(extremesky2009)040

1. Introduction

The Large Area Telescope (LAT) an board of the *Fermi Gamma Ray Space Telescope*, launched on 11 June 2008, provides unprecedented sensitivity in the γ-ray band [20 MeV to over 300 GeV] [Atwood et al. 2009] with a large increase over its predecessors EGRET [Thompson et al. 1993], and AGILE, an Italian small γ-ray astronomy mission launched in 2007 [Tavani et al.2008]. The first three months of operations in sky-survey mode led to the compilation of a list of 205 γ-ray sources with statistical significance larger than 10σ [Abdo et al. 2009a]. As largely expected from the results of EGRET and AGILE most of the high Galactic latitude sources in this catalog are blazars [Abdo et al. 2009b], a type of AGN well known to display extreme observational properties like large and rapid variability, apparent super-luminal motion, flat or inverted radio spectrum, large and variable polarization. According to a widely accepted scenario blazars are thought to be objects emitting non-thermal radiation across the entire electromagnetic spectrum from a relativistic jet that is viewed closely along the line of sight, thus causing strong relativistic amplification [e.g.[Blandford & Rees 1978, Urry & Padovani 1995]]. This strong emission at all wavelengths, makes them the dominant type of extragalactic sources in those energy windows where the accretion onto a supermassive black hole, or other thermal mechanisms, do not produce significant radiation.

One of the most effective ways of studying the physical properties of blazars is through the use of multi-frequency data. With *Fermi* , *Swift*, and other high-energy astrophysics satellites simultaneously on orbit, complemented by other space and ground-based observatories, it is now possible to assemble high-quality data to build simultaneous and well sampled SEDs of large and unbiased samples of AGN.

In [Abdo et al. 2009s] the authors have studied the broad-band (radio to high-energy γ-ray) properties of the sample of *Fermi* bright blazars presented by [Abdo et al. 2009b] making use of data coming from, over *Fermi* and *Swift*, AGILE γ-ray data, Effelsberg, OVRO, Ratan-600 1-22 GHz, radio, mm, NIR and optical data from the GASP-WEBT collaboration, Mid-infrared VISIR observations.

2. Quasi-simultaneous radio to γ-ray SEDs of 48 LBAS blazars

This sample of 48 sources is a sizable subset ($\approx$ 45%) of LBAS that is representative of the entire sample since they were chosen only on the basis of the availability of *Swift* observations (which have been scheduled largely independently of *Fermi* results) and not on brightness level or on any other condition that could influence the shape of the SED. We checked this by verifying that the distributions of redshift, optical, X-ray and γ-ray fluxes are all consistent with being the same in the two subsamples.

In all cases the overall shape of the SEDs exhibit the typical broad double hump distribution (see fig. 1), where the first bump is attributed to synchrotron radiation and the second one is likely due to one or more components related to inverse Compton emission. The dashed lines represent the best fit to the data.

The SEDs show that there are considerable differences in the position of the peaks of the two components and on their relative peak intensities. Large variability is also present, especially at

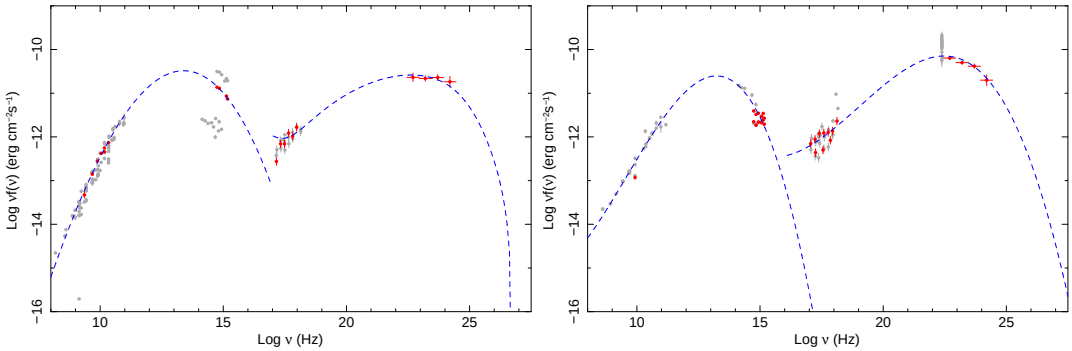

Figure 1: The SED of 0FGL J0137.1+4751 = S40133+47 (left) and of 0FGL J0210.8-5100 = PKS0208-512 (right). The quasi-simultaneous data appear as large filled red symbols, while non-simultaneous archival measurements are shown as small open grey points. The dashed lines represent the best fits to the Synchrotron and Inverse Compton part of the quasi-simultaneous SEDs (see [Abdo et al. 2009s] for detail).

optical/UV and X-ray frequencies. Gamma-ray variability cannot be evaluated as the *Fermi* data that we are using are averaged over the entire LBAS data taking period. The γ-ray variability of *Fermi* LBAS blazars is discussed in detail in a separate paper (Abdo et al. 2009, submitted).

We note that in most cases the *Fermi* data cannot be fit by a simple power law as significant curvature is detected. Downward (convex) curvature is often observed in sources where synchrotron peak is located at low energies (e.g., PKS0454-234, PKS1454-354 and PKS1502+106, 3C454.3 etc.) whereas very flat or even concave type curvature is exhibited by high synchrotron peaked objects (e.g., 3C66A, PKS 0447-439, 1ES 0502+675, and PG 1246+586). We discuss a possible explanation of these features.

3. Blazar SED observational parameters

We estimated some key observational parameters that characterize the SED of our blazars, namely, the radio spectral index (α_r), the peak frequency and peak flux of the synchrotron component ($\nu^S_{\rm peak}$and $\nu^S_{\rm peak}$F($\nu^S_{\rm peak}$)), and the peak frequency and flux of the inverse Compton part of the SED ($\nu^{IC}_{\rm peak}$and $\nu^{IC}_{\rm peak}$F($\nu^{IC}_{\rm peak}$)).

To estimate the blazar spectral slope (α_r, where $f_r(\nu) \propto \nu^{\alpha_r}$) in the radio/mm band we performed a linear regression of all the radio flux measurements that have been used for the SEDs, including the non-simultaneous ones. We conclude that the radio to micro-wave spectral slope in our SEDs is quite flat ($\langle\alpha_r\rangle \sim 0$) and consistent with being the same in all blazar types.

The $\alpha_{\rm ox}$-$\alpha_{\rm ro}$ plot of the LBAS sample is shown in Fig. 2 which also includes all blazars in the BZCat catalog [Massaro et al. 2009] for which we have radio, optical and X-ray measurements (small red dots). Note that *Fermi* FSRQs (filled circles), like all FSRQs discovered in any other energy band, are exclusively located along the top-left / bottom-right band, whereas BL Lacs (open circles) can be found in all parts of the plane, albeit with a prevalence in the horizontal area defined by values of $\alpha_{\rm ro}$ between 0.2 and 0.4, which is where HSP sources are located [Padovani & Giommi 1995]. The area of the $\alpha_{\rm ox}$-$\alpha_{\rm ro}$ space where the hypothetical population of UHSP (ultra high energy peaked) blazars [that is sources where the synchrotron component is so energetic to peak in the MeV region][Ghisellini 1999, Giommi et al. 2001] could have been

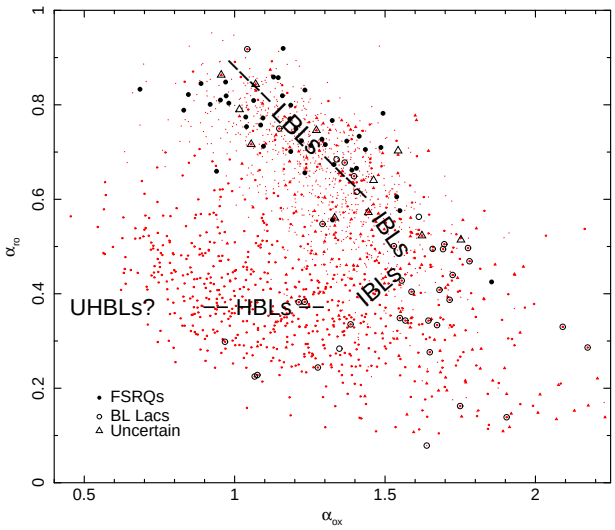

Figure 2: The α_{ox}- α_{ro} plot of the LBAS blazars (large symbols) compared to the sample of blazars in the BZCAT catalog for which there is radio optical and X-ray information (small red symbols). All gamma-ray selected blazars are located in regions covered by previously known blazars. No new γ-ray type of blazars has been found, in particular there is no evidence for the hypothetical population of Ultra High energy peaked blazars (UHSPs), with synchrotron peak in the γ-ray band ($\mathrm{Log}(\nu^S_{\mathrm{peak}}) > 10^{20}$).

found, is empty, implying that these sources are either very rare, very weak or non existent [see also][Costamante et al.2007].

3.1 An empirical method to derive ν^S_{peak} and $\nu^S_{\mathrm{peak}}\mathbf{F}(\nu^S_{\mathrm{peak}})$ from α_{ox} and α_{ro}

As shown by [Padovani & Giommi 1995], the peak of the synchrotron power ν^S_{peak} in the SED of a blazar determines its position in the α_{ox}- α_{ro} plane [Padovani & Giommi 1995], [Padovani et al. 2003]. Here we exploit this dependence showing that the value of ν^S_{peak} can be estimated from α_{ox}- α_{ro} through the following analytical relationship.

$$\mathrm{Log}(\nu_{peak_S}) = \begin{cases} 13.85 + 2.30X & if \quad \mathrm{X} < 0 \text{ and } \mathrm{Y} < 0.3 \\ 13.15 + 6.58Y & \text{otherwise} \end{cases} \tag{3.1}$$

where $\mathrm{X} = 0.565 - 1.433 \cdot \alpha_{\mathrm{ro}} + 0.155 \cdot \alpha_{\mathrm{ox}}$ and $\mathrm{Y} = 1.0 - 0.661 \cdot \alpha_{\mathrm{ro}} - 0.339 \cdot \alpha_{\mathrm{ox}}$

We have calibrated this relationship using the ν^S_{peak} values directly measured from our 48 quasi-simultaneous SED and the corresponding α_{ox} and α_{ro} values.

Comparing the values of $\mathrm{Log}(\nu^S_{\mathrm{peak}})$ estimated from equation (3.1) against the values of $\mathrm{Log}(\nu^S_{\mathrm{peak}})$ measured by fitting a SSC model to the synchrotron part of the quasi-simultaneous SEDs, we obtain a distribution of the difference between the values estimated with the two methods which has a mean value of 0.04 and a standard deviation of 0.58, implying that the value of $\mathrm{Log}(\nu^S_{\mathrm{peak}})$ can be derived even from non-simultaneous values of α_{ox} and α_{ro} within 0.6 decade at one sigma level and within 1 decade in almost all cases.

It must be noted, however, that this method assumes that the optical and X-ray fluxes are not contaminated by thermal emission from the disk or accretion. In blazars where thermal flux components are not negligible (this should probably occur more frequently in low radio luminosity

sources) the method described above may lead to a significant overestimation of the position of $\nu^S_{\rm peak}$.

The peak flux $\nu^S_{\rm peak}{\rm F}(\nu^S_{\rm peak})$ can be estimated using the following relationship

$$\mathrm{Log}(\nu_{peak_S} F(\nu_{peak_S})) = 0.5 \cdot \mathrm{Log}(\nu_{peakS}) - 20.4 + 0.9 \cdot \mathrm{Log}(\mathrm{R_{5GHz}}), \quad (3.2)$$

where $\mathrm{R_{5GHz}}$ is the radio flux density at 5 GHz in units of mJy.

Also in this case the comparison of the value of $\nu^S_{\rm peak}{\rm F}(\nu^S_{\rm peak})$ estimated with the two methods is very good with an average value of -0.01 for the difference between the two estimates and a standard deviation of 0.33.

It is quite remarkable that one can derive the synchrotron peak flux simply from $\nu^S_{\rm peak}$and from the radio flux as this implies that within a factor of 10 the radio emission represents a long-term calorimeter for the whole jet activity and the basic source power.

3.2 The peak frequency and peak intensity of the inverse Compton bump

We have estimated the peak of the inverse Compton power in the SED ($\nu^{IC}_{\rm peak}$) and the corresponding peak flux ($\nu^{IC}_{\rm peak}{\rm F}(\nu^{IC}_{\rm peak})$) by fitting the X-ray to γ-ray part of the SED, which is dominated by inverse Compton emission using a third degree polynomial function.

There are some objects in which the soft X-ray band is still dominated by synchrotron radiation, and only the *Fermi* data can be used to constrain the inverse Compton component, so the above method is subject to large uncertainties. For this reason, in these cases, we have used the ASDC SED [1] interface to fit the simultaneous data points to a SSC model with a log-parabolic electron spectrum [Tramacere 2009].

For the whole sample we have determined $\nu^{IC}_{\rm peak}$as the value of ν which maximizes νF_ν in polynomial function or the predictions of the SSC model. The best fit to both the synchrotron and inverse Compton components appear as dashed lines in Fig. 1.

Fig. 3 (right panel) shows that the $\nu^{IC}_{\rm peak}$, derived as described above for the 48 sources for which we have built the SEDs, is strongly correlated with their γ-ray spectral slope (Γ) taken from Table 3 of [Abdo et al. 2009b].

We note that the scatter in the plots of Fig. 3 is largest in the regions of low $\nu^S_{\rm peak}/\nu^{IC}_{\rm peak}$- steep values of Γ, probably reflecting the presence of γ-ray spectral curvature. The best fit to the $\nu^{IC}_{\rm peak}$–Γ relationship is

$$Log(\nu^{IC}_{\rm peak}) = -4.0 \cdot \Gamma + 31.6 \quad (3.3)$$

Since the 48 objects for which we have quasi-simultaneous SEDs are representative of the entire LBAS sample the above equation can be used to estimate the $\nu^{IC}_{\rm peak}$of the LBAS sources for which we have no simultaneous SEDs. The statistical uncertainty associated to $\nu^{IC}_{\rm peak}$calculated via eq. 3.3 can be estimated from the distribution of the difference between $\nu^{IC}_{\rm peak}$measured from the SED and that from eq. 3.3. This distribution is centered on the value of 0 and has a sigma of 0.51; considering that the value of $\nu^{IC}_{\rm peak}$from the SED is also subject to a similar error we conservatively conclude that the Log of $\nu^{IC}_{\rm peak}$values estimated through eq. 3.3 has an associated error of about 0.7.

[1] http://tools.asdc.asi.it/SED/

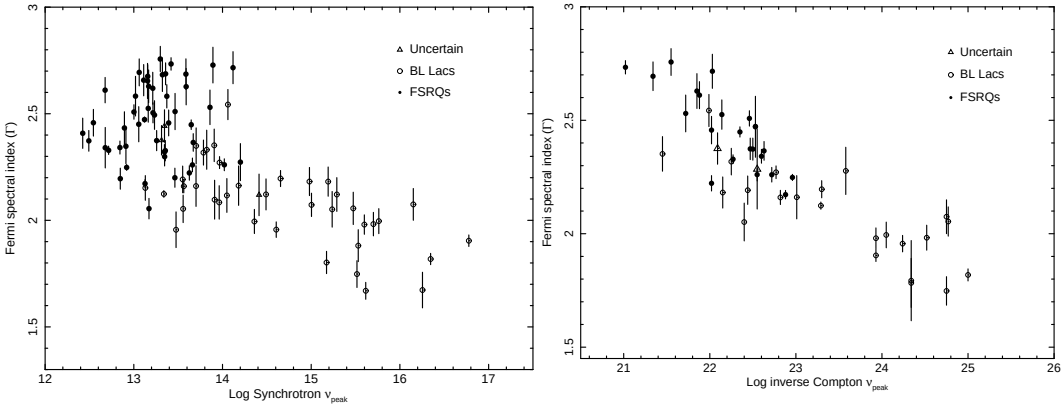

Figure 3: The γ-ray power law photon spectral index (Γ) is plotted against the log of synchrotron peak energy (left panel) and the Log of inverse Compton peak energy (right panel). A clear correlation is present in both cases. Note that BL Lacs behave differently than FSRQs spanning a wider range of both $\nu^S_{\rm peak}$and spectral slopes.

Ideally, blazars should be classified on the basis of a complete SED built with simultaneous data. As in most cases this is not possible, **LSP** or *Low Synchrotron Peaked* blazars or **HSP** or *High Synchrotron Peaked* blazars can still be recognized by estimating their $\nu^S_{\rm peak}$from $\alpha_{\rm ox}$ and $\alpha_{\rm ro}$ and from their X-ray spectral shape or by their radio to X-ray spectral slope [Padovani et al. 2003].

In LSP sources the X-ray spectrum is flat (photon spectral index $1.5 < \gamma_{\rm x} < 1.8$) and dominated by the IC component. In HSP sources the X-ray spectrum is instead still due to synchrotron emission and it is usually steep ($\gamma_{\rm x} > 2$) if $\nu^S_{\rm peak} \lesssim 10^{17} Hz$ but it can still be flat in extreme HSPs where $\nu^S_{\rm peak}$is well into the X-ray band; the radio to X-ray spectral index, α_{rx} of these blazars is less than 0.7. In **ISP** or *Intermediate Synchrotron Peaked* blazars both the (steep) tail of the synchrotron emission and the (flat) rise of the IC component are within the X-ray band (see figure 4), and $0.7 \lesssim \alpha_{rx} \lesssim 0.8$.

3.3 The distribution of synchrotron and inverse Compton peak frequencies

Having a new SED-based classification of blazars and a reliable method of estimating $\nu^S_{\rm peak}$we inspect the LBAS sample in terms of its content of LSP, ISP, and HSP objects and we compared it with that of samples selected in other energy bands.

The distribution of the synchrotron peak frequency ($\nu^S_{\rm peak}$) of LBAS blazars (estimated using the $\alpha_{\rm ox}$- $\alpha_{\rm ro}$ method) shows that while the $\nu^S_{\rm peak}$distribution of FSRQs starts at $\sim 10^{12.5}$ Hz, peaks at $\sim 10^{13.3}$ Hz and it does not extend beyond $\approx 10^{14.5}$ Hz, the distribution of BL Lacs is much flatter, starts at $\sim 10^{13}$ Hz and reaches much higher frequencies ($\approx 10^{17}$ Hz) than that of FSRQs.

We compare this result with the distribution of $\nu^S_{\rm peak}$of the sample of FSRQs and BL Lacs detected as foreground sources in the WMAP 3-year microwave anisotropy maps [Giommi et al. 2009] and with the $\nu^S_{\rm peak}$distribution of the LBAS sample with that of the X-ray selected sample of blazars detected in the *Einstein* Extended Medium Sensitivity Survey [EMSS, [Gioia et al. 1990]].

We see that the $\nu^S_{\rm peak}$distribution of FSRQs is consistent with being the same in the γ-ray, radio/microwave and in the X-ray band. We note that the large majority of FSRQs are of the LSP type while no FSRQs of the HSP type have been found at any frequency. On the contrary, the

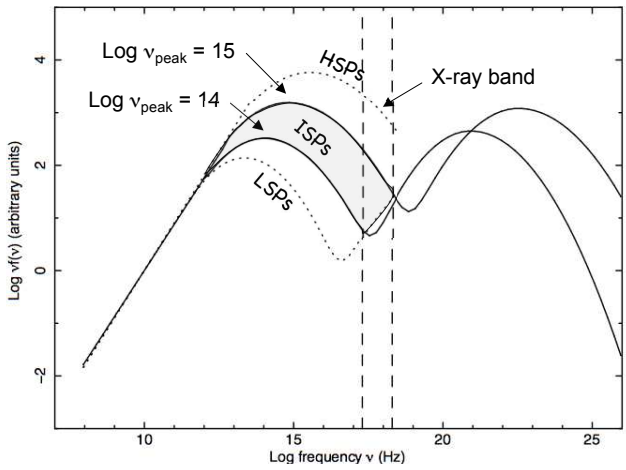

Figure 4: The definition of different blazar types based on the peak of the synchrotron component ($\nu^S_{\rm peak}$) in their SED. Low Synchrotron Peaked blazars, or LSP are those where $\nu^S_{\rm peak}$is located at frequencies lower then 10^{14} Hz (e.g., lower dotted line), for Intermediate Synchrotron Peaked sources, or IPB, 10^{14} Hz $< \nu_{peak_S} < 10^{15}$ Hz, (SEDs with peak within the grey area) while for High Synchrotron Peaked blazars, or HPS, $\nu^S_{\rm peak} > 10^{15}$ Hz (e.g., upper dotted line).

$\nu^S_{\rm peak}$distribution of BL Lac objects is very different in the three energy bands. It is strongly peaked at $\sim 10^{13.3}$ Hz in the microwave band, where HSP sources are very rare, whereas in the X-ray and γ-ray bands HSP sources are more abundant than LSPs.

Looking at the distribution of the inverse Compton peak frequency, $\nu^{IC}_{\rm peak}$, of the FSRQs and the BL Lacs in the LBAS sample, we note that they are quite different with the BL Lacs exhibiting much higher $\nu^{IC}_{\rm peak}$values.

This is most likely due to the same reason that causes the different $\nu^S_{\rm peak}$distributions in the two blazar subclasses.

4. Conclusion

We derived reliable estimates of the frequency of the synchrotron ($\nu^S_{\rm peak}$) and of the inverse Compton peaks ($\nu^{IC}_{\rm peak}$) for over 100 LBAS blazars, both directly from the simultaneous data and indirectly using a refined version of the method of [Padovani & Giommi 1995] based on the position in the $\alpha_{\rm ox}$- $\alpha_{\rm ro}$ plane, for the former, and on the slope of the γ-ray spectrum for the latter, as the γ-ray spectral slope and $\nu^{IC}_{\rm peak}$are strongly correlated (see Fig.3).

Among the several results we obtained, we can conclude that gamma-ray selected blazars have broad-band spectral properties similar to those of radio and X-ray discovered blazars implying

that they are all drawn from the same underlying population; the distribution of the synchrotron peak frequency is very different for the FSRQ and BL Lac subsamples. The results rule out the existence of FSRQs of the HSP type , consistent with what also observed in radio, microwave and X-ray surveys; the BL Lac minimum $\nu^S_{\rm peak}$appears to be larger than in FSRQs and this could be due to some intrinsic difference in the mechanism of particle acceleration in the two types of blazars or to a mere selection effect; a simple homogeneous, one-zone, SSC model cannot explain the SED of the majority of the detected sources, especially of the LBL type (see A. Tramacere proceeding of this conference). In addition, differential variability in the simultaneous optical and X-ray data observed in ISP and HSP objects (that is close to the peak of the synchrotron component) suggests that multiple components are present in non LSP blazars [e.g., S5 0716+714, [Giommi et al. 2008]] as also clearly shown by simultaneous X-ray/TeV campaigns [e.g., PKS 2155-304, [Aharonian et al. 2009]].

References

[Abdo et al. 2009a] Abdo, A.A. et al, 2009a, ApJS,183, 46

[Abdo et al. 2009b] Abdo, A.A. et al, 2009b, ApJ, 700, 597

[Abdo et al. 2009s] Abdo, A.A. et al, submitted to ApJ

[Aharonian et al. 2009] Aharonian, F. et al. 2009, ApJ 696L, 150

[Atwood et al. 2009] Atwood, W. B., et al. 2009, ApJ, 697, 1071

[Blandford & Rees 1978] Blandford, R.D. & Rees, M.J. 1978, in Pittsburg Conference on BL Lac Objects, Ed. A.M. Wolfe, Pittsburgh, University of Pittsburgh press, p. 328

[Costamante et al.2007] Costamante, L., Aharonian, F. & Khangulyan D., 2007, AIPC, 921,157

[Gioia et al. 1990] Gioia, I. M., Maccacaro, T., Schild, R. E., Wolter, A., Stocke, J. T., Morris, S. L., Henry, J. P., 1990 ApJS, 72, 576

[Ghisellini 1999] Ghisellini, G. 1999, ApL&C, 39, 17

[Giommi et al. 2001] Giommi, P., Ghisellini, G., Padovani, P., & Tagliaferri, G., 2001, AIPC, 599, 441

[Giommi et al. 2009] Giommi, P., et al. 2009 A&A, 508, 107-115, 2009

[Giommi et al. 2008] Giommi, P., et al. 2008, A&A 487, L49

[Massaro et al. 2009] Massaro, E., Giommi, P., Leto, C., Marchegiani, P., Maselli, A., Perri, M., Piranomonte, S., Sclavi, S., 2009 AA, 495, 691

[Padovani & Giommi 1995] Padovani, P. & Giommi, P., 1995, ApJ, 444, 567

[Padovani et al. 2003] Padovani, P., Perlman, E.S., Landt, E., Giommi, P., Perri, M., 2003, ApJ, 588, 128

[Tavani et al.2008] Tavani, M., Barbiellini, G., Argan, A. et al. 2008, Nucl. Instr. and Meth. in Phys. Res. A, 588, 52

[Thompson et al. 1993] Thompson, D. J. et al. 1993 ApJS, 86, 629

[Tramacere 2009] Tramacere, A. et al., 2009, A&A, 501, 879

[Urry & Padovani 1995] Urry, M. & Padovani, P. 1995, PASP, 107, 803